Model Reference Control of Constrained Overactuated Systems with Integral Compensation

Grégoire Le Goff, Marc Bodson, Maurice Fadel

Model Reference Control of Constrained Overactuated Systems with Integral Compensation

Grégoire Le Goff, Marc Bodson and Maurice Fadel

***Abstract*—A model reference control allocation (CA) method is modified to become a control allocation method with integrator (CAI), it significantly improves control performance while readily integrating with existing methods. In general, CA methods take advantage of the redundancy of an overactuated system to achieve control objectives while respecting actuator limits. The method of this paper adds integral compensation to a CA method for multivariable model reference control with the special property that the closed-loop behavior remains the same. The transfer function matrix is preserved, yet zero static error results when experiencing small parametric uncertainties and constant disturbances. The application of the concept to the coordinated control of multiple buck converters feeding a common load is considered. A simulation of the system confirms the benefits of the proposed method.**

***Index Terms*—Model Reference Control, Control Allocation, Integrator, Online Optimization, Control Method**

I. Introduction

The objective of control allocation (CA) methods is to take advantage of multiple control variables in order to optimally operate a system while respecting actuator limits. First developed in the aeronautical domain [1], [2], CA methods were proposed to exploit redundant control surfaces for flight control. The application fields of CA methods developed and diversified [3]–[8], and now include power electronic converters [9], [10]. Control allocation methods are envisioned for converters with a very large number of switches (i.e. control variables), such as the modular multilevel converter (MMC) [11], [12].

CA methods available in the literature are based on solving an *allocation equation*, and can be divided into three main categories: 1) Model-Inversion-Based (MIB) [3], [13], [14]; 2) Error Minimization Online (EMOn) [4], [6], [15], [16]; and 3) Error Minimization Offline (EMOff) [5], [7], [8]. The allocation equation of this paper extends the multivariable model reference control law proposed in [4] for flight control and adapted to discrete-time. With the algorithm from [4], the closed-loop response matches the response of a desired model. However, small uncertainties and input disturbances lead to tracking errors. The method proposed in this paper eliminates such errors by incorporating integral compensation. A remarkable property of the scheme is that the same closed-loop response is achieved with a minor modification of the algorithm.

The addition of an integrator in control laws using CA was considered in [10], [17]–[19]. However, the result was achieved by cascading two control loops: a controller with an integrator is in charge of an outer control loop and the inner loop involves the control allocation. Compared to these works, the novelty of the approach presented here is the implementation of an integrator into the control method and without inducing any changes in the closed-loop dynamic behavior.

To summarize, the main contributions of the paper are:

- Addition of an integral action that eliminates the static error and rejects constant disturbances. Those capabilities are shown to hold also under small parametric uncertainties
- The integral compensation added is transparent, meaning that the input/output response remains unchanged
- This enhancement of the CA is readily implemented: it can be seamlessly integrated with any existing CA algorithm
- The disturbance rejection response can be tuned to obtain different dynamics than those of the reference model

The paper is organized as follows. The original formulation of the CA method is reviewed in Section II-A. In Section II-B, the control allocation method with integrator (CAI) is presented and its characteristics are analyzed. A comparison of CA vs. CAI is conducted in Section II-C. The benefits of CAI over CA are demonstrated using the simulation of a system involving multiple power electronic converters in Section III.

II. Derivation of the Model Reference Control Allocation Method with Integrator

A. Original CA architecture

The system to be controlled is defined by the following discrete-time state-space model:

$$\mathbb{S} \triangleq \begin{cases} \mathbf{X}_{k+1} = F\mathbf{X}_k + G\mathbf{U}_k + H\mathbf{E}_k \\ \mathbf{Y}_k = C\mathbf{X}_k \end{cases} \tag{1}$$

where $\mathbf{X}_k \in \mathbb{R}^{n_x}$ is the state vector, $\mathbf{U}_k \in \mathbb{R}^{n_u}$ is the control vector, $\mathbf{Y}_k \in \mathbb{R}^{n_y}$ is the output vector, $\mathbf{E}_k \in \mathbb{R}^{n_x}$

This work was not supported by any organization.

Grégoire Le Goff and Maurice Fadel are with the LAPLACE, Université de Toulouse, CNRS, INPT, UPS, Toulouse, France legoff@laplace.univ-tlse.fr, fadel@laplace.univ-tlse.fr

Marc Bodson is with the Department of Electrical and Computer Engineering, University of Utah, Salt Lake City, Utah, USA marc.bodson@utah.edu

is a known additive perturbation (possibly due to nonlinearity of the system), and $F \in \mathbb{R}^{n_x \times n_x}$, $G \in \mathbb{R}^{n_x \times n_u}$, $C \in \mathbb{R}^{n_y \times n_x}$, are the dynamic matrix, the control matrix and the observation matrix, respectively. Combining the equations of (1) together leads to:

$$\mathbf{Y}_{k+1} = C\left(F\mathbf{X}_k + H\mathbf{E}_k\right) + CG\mathbf{U}_k \tag{2}$$

Let (3) describe the reference model that specifies the desired response of the system in closed-loop:

$$\mathbf{Y}^*_{k+1} = F_M\mathbf{Y}_k + (\mathbb{I}_{n_y} - F_M)\mathbf{Y}^{ref}_k \tag{3}$$

where $F_M \in \mathbb{R}^{n_y \times n_y}$ is the dynamic matrix specifying the poles of the reference model and $\mathbb{I}_{n_y} - F_M$ is its control matrix chosen to ensure unit static gain. The control $\mathbf{U}_k$ ensuring that $\mathbf{Y}_{k+1}$ matches $\mathbf{Y}^*_{k+1}$ is such that:

$$\begin{aligned} CG\ \mathbf{U}_k = & \left[F_M\mathbf{Y}_k + (\mathbb{I}_{n_y} - F_M)\mathbf{Y}^{ref}_k\right] - C\left(F\mathbf{X}_k + H\mathbf{E}_k\right) \\ \iff \quad & M\ \mathbf{U}_k = \mathbf{a_d}_k \end{aligned} \tag{4}$$

with

$$\mathbf{a_d}_k = \left[F_M\mathbf{Y}_k + (\mathbb{I}_{n_y} - F_M)\mathbf{Y}^{ref}_k\right] - C\left(F\mathbf{X}_k + H\mathbf{E}_k\right) \in \mathbb{R}^{n_a} \tag{5}$$

where $\mathbf{a_d}_k$ is the desired action vector representing the control objective and $M = CG \in \mathbb{R}^{n_a \times n_u}$ is the allocation matrix representing the effectiveness of the control variables contained in $\mathbf{U}_k$ to the achievement of the desired action vector $\mathbf{a_d}_k$. Thus the control allocation problem to be solved can be written as:

$$\{M\ \mathbf{U}_k = \mathbf{a_d}_k \mid \mathbf{U}_{min} \leq \mathbf{U}_k \leq \mathbf{U}_{max}\} \tag{6}$$

where $\mathbf{U}_{min}$ and $\mathbf{U}_{max}$ are the control boundaries. Equation (4) is called the *allocation equation* and CA methods (MIB, EMOn, EMOff) are all based on solving a problem of the form of (6). In real time, solving (6) can be conceptually divided into two blocks:

- A first block $\mathbb{P}$ for *Preparation* that will update the value of $\mathbf{a_d}_k$ at each time step and M in case the considered system is nonlinear or temporally varying and requires an update of M. The model of the system used in order to compute $\mathbf{a_d}_k$ can also adapt to system variations, which means that the control system is capable of reconfiguration.
- A second block $\mathbb{A}$ for *Allocation* that will determine $\mathbf{U}_k$ from the knowledge of M and $\mathbf{a_d}_k$, using a method from one of the three CA families (MIB, EMOn or EMOff).

The block diagram decomposition is shown in Fig. 1 (a) with $\mathbb{S}$ representing the open-loop system to be controlled as defined by (1).

About the *Allocation* part, for example using EMOn, an online optimization computation takes place to minimize a criterion depending on the allocation error $\mathbf{e}_k = M\mathbf{U}_k - \mathbf{a_d}_k$ and under the constraint of the control boundaries: $\mathbf{U}_{min} \leq \mathbf{U}_k \leq \mathbf{U}_{max}$. Different optimization criteria have been considered ([3], [4]), but a general formulation consists in solving (omitting the subscript k for simplicity):

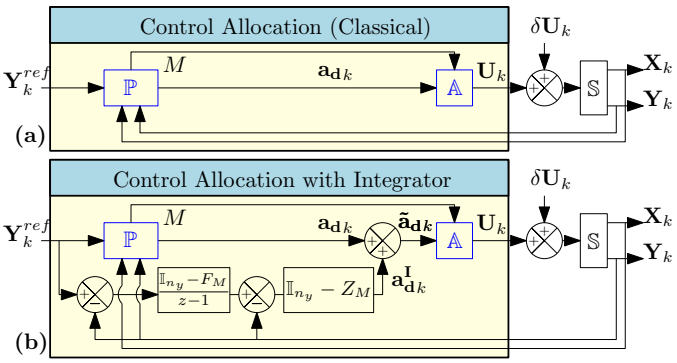

Fig. 1. (a) Control Allocation (CA) using the original architecture. (b) the novel model reference Control Allocation with Integrator (CAI) architecture. Common blocks to both architectures are in blue.

$$\begin{cases} \min_{\mathbf{U},\mathbf{e}} J_l = ||\mathbf{e}||_l^l \\ \textit{such that :} \\ M\ \mathbf{U} - \mathbf{e} = \mathbf{a_d} \\ \mathbf{U}_{min} \leq \mathbf{U} \leq \mathbf{U}_{max} \\ -\mathbf{e}_{max} \leq \mathbf{e} \leq \mathbf{e}_{max} \end{cases} \tag{7}$$

where $\mathbf{e}_{max}$ is an upper bound on the achievable error and l is a given norm to be chosen. For example, [4], [6], [20] use the $l1$-norm, [6] uses the $l\infty$-norm, and [6], [16] use the $l2$-norm. To analyze the dynamics of the system away from saturation of the control variables, the following assumption is made.

Assumption 1. *The Allocation block $\mathbb{A}$ in Fig. 1 (a) guarantees the verification of* (4) *at any time. Let $M\ \mathbf{U}_k = \mathbf{a_d}_k$ be true for all time step k.*

Assuming that Assumption 1 is satisfied, the following result is obtained.

Theorem 1. *The transfer function matrix linking $\mathbf{Y}^{ref}$ to $\mathbf{Y}$ in closed-loop is $T_{CL}(z) = \left[z\mathbb{I}_{n_y} - F_M\right]^{-1}(\mathbb{I}_{n_y} - F_M)$. The closed-loop dynamics are of order n_y and are governed by the F_M dynamic matrix of the reference model* (3)*. This matrix specifies the poles in closed-loop and no zero influences the dynamics.*

Proof 1. *Assumption 1 holding true, substituting $CG\ \mathbf{U}_k$ for $M\ \mathbf{U}_k$ from* (4) *in* (2) *gives:*

$$\mathbf{Y}_{k+1} = C(F\mathbf{X}_k + H\mathbf{E}_k) + \mathbf{a_d}_k = F_M\mathbf{Y}_k + (\mathbb{I}_{n_y} - F_M)\mathbf{Y}^{ref}_k \tag{8}$$

By applying the z-transform with zero initial conditions, this equation becomes:

$$\left[z\mathbb{I}_{n_y} - F_M\right]\mathbf{Y}(z) = (\mathbb{I}_{n_y} - F_M)\mathbf{Y}^{ref}(z) \tag{9}$$

Thus, the closed-loop transfer function matrix is obtained:

$$T_{CL}(z) = \left[z\mathbb{I}_{n_y} - F_M\right]^{-1}(\mathbb{I}_{n_y} - F_M) \tag{10}$$

■

Equation (10) shows that the closed-loop behavior is the one of the reference model, which means having n_y poles and no zero in closed-loop.

Theorem 2. *The transfer function matrix relating a control disturbance $\delta\mathbf{U}$ to $\mathbf{Y}$ in closed-loop is $T_{SU}(z) = \left[z\mathbb{I}_{n_y} - F_M\right]^{-1} M$. In general, constant disturbances are not rejected.*

Proof 2. *To perform the sensitivity function analysis, $\mathbf{Y}^{ref}$ is set to zero and $\mathbf{U}$ is increased by a disturbance $\delta\mathbf{U}$. Equation* (2) *becomes:*

$$\mathbf{Y}_{k+1} = C\left(F\mathbf{X}_k + H\mathbf{E}_k\right) + M\ \mathbf{U}_k + M\ \delta\mathbf{U}_k \tag{11}$$

Substituting $M\mathbf{U}_k$ by its expression from (4) *with a null $\mathbf{Y}^{ref}$ gives:*

$$\mathbf{Y}_{k+1} = F_M\mathbf{Y}_k + M\ \delta\mathbf{U}_k \tag{12}$$

Therefore, the z-transform of (12) *leads to:*

$$\left[z\mathbb{I}_{n_y} - F_M\right]\mathbf{Y}(z) = M\ \delta\mathbf{U}(z) \tag{13}$$

The sensitivity function can then be deduced to be:

$$T_{SU}(z) = \left[z\mathbb{I}_{n_y} - F_M\right]^{-1} M \tag{14}$$

■

B. The novel CAI architecture

The method with integrator provides the *Allocation* block with a problem of the form (6) to solve, but including integral compensation.

Definition 1. *The novel control allocation method with integrator (CAI) is defined by:*

$$\begin{cases} M\ \mathbf{U}_k = \mathbf{a_d}_k + \mathbf{a}^{\mathbf{I}}_{\mathbf{d}k} = \tilde{\mathbf{a}}_{\mathbf{d}k} \\ \mathbf{a_d}_k = \left[F_M\mathbf{Y}_k + (\mathbb{I}_{n_y} - F_M)\mathbf{Y}^{ref}_k\right] - C\left(F\mathbf{X}_k + H\mathbf{E}_k\right) \\ \mathbf{a}^{\mathbf{I}}_{\mathbf{d}k} = \left(\mathbb{I}_{n_y} - Z_M\right)\left[\left(\mathbb{I}_{n_y} - F_M\right)\mathbf{X}_{\mathbf{r}k} - \mathbf{Y}_k\right] \\ \mathbf{X}_{\mathbf{r}k+1} = \mathbf{X}_{\mathbf{r}k} + \left(\mathbf{Y}^{ref}_k - \mathbf{Y}_k\right) \end{cases} \tag{15}$$

where $Z_M \in \mathbb{R}^{n_y \times n_y}$ and the output of the integrator $\mathbf{X_r} \in \mathbb{R}^{n_y}$.

Compared to (4), the vector $\mathbf{a}^{\mathbf{I}}_{\mathbf{d}k}$ in (15) is added to $\mathbf{a_d}_k$ in order to bring the integral action into the allocation equation. The allocation equation thus replaces $\mathbf{a_d}_k$ from the original CA to $\tilde{\mathbf{a}}_{\mathbf{d}k}$ for the CAI. With the addition of the integral compensation, the core structure of the control allocation is retained, which means having a problem of the form (6) to solve. The CAI can then be represented by Fig. 1 (b), compared to the original CA in Fig. 1 (a).

C. CAI characteristics and comparison with CA

The characteristics of the CAI method are discussed in this section, Theorem 3 describes the reference tracking closed-loop behavior, Theorem 4 describes the disturbance rejection closed-loop behavior, and Theorem 5 gives the static error in closed-loop. In order to analyze the linear behavior (away from saturation), the following assumption is made.

Assumption 2. *The Allocation block $\mathbb{A}$ in Fig. 1 (b) guarantees that $M\ \mathbf{U}_k = \tilde{\mathbf{a}}_{\mathbf{d}k}$ is satisfied for all time.*

Theorem 3. *The transfer function matrix linking $\mathbf{Y}^{ref}$ to $\mathbf{Y}$ in closed-loop is $\tilde{T}_{CL}(z) = \left[z\mathbb{I}_{n_y} - F_M\right]^{-1}\left(\mathbb{I}_{n_y} - F_M\right)$. The closed-loop dynamics for the system using CAI are of order n_y and are governed by the F_M dynamic matrix of the reference model* (3) *with the condition that the eigenvalues of Z_M are chosen to be stable and well-damped. Ultimately the matrix F_M specifies the poles in closed-loop and no zero influences the dynamics.*

Proof 3. *Assumption 2 holding true, substituting CG $\mathbf{U}_k$ for $M\ \mathbf{U}_k$ from* (15) *in* (2) *gives:*

$$\begin{aligned} \mathbf{Y}_{k+1} &= C(F\mathbf{X}_k + H\mathbf{E}_k) + \tilde{\mathbf{a}}_{\mathbf{d}k} \\ &= F_M\mathbf{Y}_k + (\mathbb{I}_{n_y} - F_M)\mathbf{Y}^{ref}_k + \mathbf{a}^{\mathbf{I}}_{\mathbf{d}k} \end{aligned} \tag{16}$$

By applying the z-transform with zero initial conditions:

$$\left[z\mathbb{I}_{n_y} - F_M\right]\mathbf{Y}(z) = (\mathbb{I}_{n_y} - F_M)\mathbf{Y}^{ref}(z) + \mathbf{a}^{\mathbf{I}}_{\mathbf{d}}(z) \tag{17}$$

Applying the z-transform to the third and fourth equations of system (15) *gives:*

$$\begin{cases} \mathbf{a}^{\mathbf{I}}_{\mathbf{d}}(z) = \left(\mathbb{I}_{n_y} - Z_M\right)\left[\left(\mathbb{I}_{n_y} - F_M\right)\mathbf{X_r}(z) - \mathbf{Y}(z)\right] \\ \mathbf{X_r}(z) = (z-1)^{-1}\left(\mathbf{Y}^{ref}(z) - \mathbf{Y}(z)\right) \end{cases} \tag{18}$$

First substituting $\mathbf{X_r}(z)$ from (18) *into $\mathbf{a}^{\mathbf{I}}_{\mathbf{d}}(z)$ from* (18)*, and then substituting $\mathbf{a}^{\mathbf{I}}_{\mathbf{d}}(z)$ into* (17)*, one finds:*

$$\begin{aligned} &\left[z\mathbb{I}_{n_y} - Z_M\right]\left[z\mathbb{I}_{n_y} - F_M\right]\mathbf{Y}(z) \\ &= \left[z\mathbb{I}_{n_y} - Z_M\right]\left(\mathbb{I}_{n_y} - F_M\right)\mathbf{Y}^{ref}(z) \end{aligned} \tag{19}$$

Note that cancellations of the $z\mathbb{I}_{n_y} - Z_M$ terms on both sides of the equation is possible under the condition that the eigenvalues of Z_M are chosen to be stable and well-damped. After cancellations, the closed-loop transfer function is derived:

$$\tilde{T}_{CL}(z) = \left[z\mathbb{I}_{n_y} - F_M\right]^{-1}\ \left(\mathbb{I}_{n_y} - F_M\right) \tag{20}$$

■

Equation (20) shows that the closed-loop behavior is the same as that of the reference model, which means having n_y poles and no zero in closed-loop.

Corollary 1. *The closed-loop reference tracking behavior of the system is the same whether one uses CA or CAI. Adding the integral compensation is transparent for the reference tracking,*

as $T_{CL}(z) = \tilde{T}_{CL}(z)$. Since $\tilde{T}_{CL}(z)$ is obtained from a pole-zero cancellation, CA and CAI will have the same behavior in closed-loop under the assumption made that the eigenvalues of Z_M are chosen to be stable and well-damped. If CA and CAI do not have the same initial conditions, the difference between the responses will converge to zero exponentially with a tunable time constant.

Although the closed-loop tracking response is the same, the response to input disturbances is modified, as shown in the following theorem.

Theorem 4. *The transfer function matrix relating a control disturbance $\delta\mathbf{U}$ to $\mathbf{Y}$ in closed-loop is $\tilde{T}_{SU}(z) = \left[z\mathbb{I}_{n_y} - F_M\right]^{-1}\left[z\mathbb{I}_{n_y} - Z_M\right]^{-1}(z-1)M$. Therefore, with CAI, the disturbance rejection dynamics are governed by the matrices F_M and Z_M.*

Proof 4. *To perform the sensitivity function analysis, $\mathbf{Y}^{ref} = \mathbf{0}$ and $\mathbf{U}$ is increased by a disturbance $\delta\mathbf{U}$. Equation* (2) *becomes:*

$$\mathbf{Y}_{k+1} = C\left(F\mathbf{X}_k + H\mathbf{E}_k\right) + M\ \mathbf{U}_k + M\ \delta\mathbf{U}_k \tag{21}$$

Substituting $M\mathbf{U}_k$ by its expression from (15) *with zero $\mathbf{Y}^{ref}$ gives:*

$$\mathbf{Y}_{k+1} = F_M\mathbf{Y}_k + \mathbf{a}^{\mathbf{I}}_{\mathbf{d}k} + M\ \delta\mathbf{U}_k \tag{22}$$

Keeping the reference null, (18) *is updated to:*

$$\mathbf{a}^{\mathbf{I}}_{\mathbf{d}}(z) = -\left(\mathbb{I}_{n_y} - Z_M\right)\left[\left(\mathbb{I}_{n_y} - F_M\right)(z-1)^{-1} + \mathbb{I}_{ny}\right]\mathbf{Y}(z) \tag{23}$$

Therefore, the z-transform of (22) *taking into account* (23) *leads to:*

$$\left[z\mathbb{I}_{n_y} - F_M\right]\left[z\mathbb{I}_{n_y} - Z_M\right]\mathbf{Y}(z) = (z-1)M\ \delta\mathbf{U}(z) \tag{24}$$

The sensitivity function can then be deduced to be:

$$\tilde{T}_{SU}(z) = \left[z\mathbb{I}_{n_y} - F_M\right]^{-1}\left[z\mathbb{I}_{n_y} - Z_M\right]^{-1}(z-1)M \tag{25}$$

■

Theorem 5. *The use of the CAI control architecture ensures zero static error and input-matched disturbance rejection for a step-input disturbance: $\varepsilon_{\mathbf{s}} = \mathbf{0}$ for $\mathbf{y}^{ref}(t) = \mathcal{H}(t)\ \mathbf{Y_0} \in \mathbb{R}^{n_y}$ and $\delta\mathbf{u}(t) = \mathcal{H}(t)\ \delta\mathbf{U_0} \in \mathbb{R}^{n_u}$ where $\mathcal{H}(t)$ is the Heaviside step function. $\mathbf{Y_0}$ and $\delta\mathbf{U_0}$ are vectors containing constant components over time.*

Proof 5. *For a step-input reference $\mathbf{y}^{ref}(t) = \mathcal{H}(t)\ \mathbf{Y_0}$, the z-transform gives $\mathbf{Y}^{ref}(z) = z\ \mathbf{Y_0}\ (z-1)^{-1}$. For a step-input disturbance $\delta\mathbf{u}(t) = \mathcal{H}(t)\ \delta\mathbf{U_0}$, the z-transform brings $\delta\mathbf{U}(z) = z\ \delta\mathbf{U_0}\ (z-1)^{-1}$. From Theorems 3 and 4, the system being linear and using the superposition principle, $\mathbf{Y}(z)$ can thus be derived:*

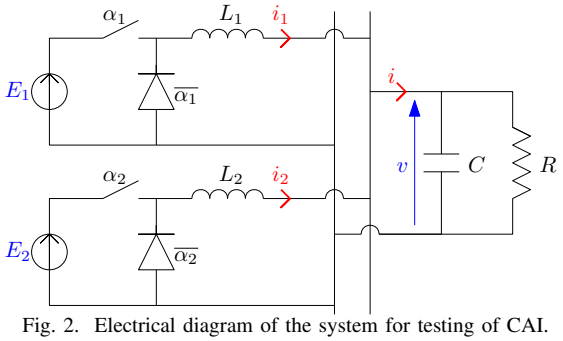

Fig. 2. Electrical diagram of the system for testing of CAI.

$$\mathbf{Y}(z) = \tilde{T}_{CL}(z)\ \mathbf{Y}^{ref}(z) + \tilde{T}_{SU}(z)\ \delta\mathbf{U}(z) \tag{26}$$

By the final value theorem, the static error is derived:

$$\begin{aligned}\varepsilon_{\mathbf{s}} &= \lim_{z\to 1}(z-1)\left(\mathbf{Y}^{ref}(z) - \mathbf{Y}(z)\right)\\ &= \left[(\mathbb{I}_{n_y} - \mathbb{I}_{n_y})\mathbf{Y_0} - (0)M\delta\mathbf{U_0}\right] = \mathbf{0}\end{aligned} \tag{27}$$

■

According to Theorem 5, the proposed method removes the static error and ensures input-matched disturbance rejection. The presence of the integral compensation ensures that the static error remains zero even if there are parametric errors that are small enough to preserve the stability of the closed-loop system. Through Theorems 3 and 4, Theorem 5 assumes that the output reference setpoint lies within the feasible operating zone of the system. If the output reference setpoint requires the control to exceed its limits in steady-state, Assumption 2 will no longer hold and the static error and disturbance may not be rejected.

III. Simulations

A. Description and model of the system

The system under consideration is composed of two buck converters feeding a common load, as shown on Fig. 2. Each buck converter is capable of delivering a current up to some maximum value, and the load requires a specified total current. The system is a good example of an overactuated system suitable for the use of control allocation methods. The work of [10] presents a control architecture for this converter and a model that will be used here. The control objectives of this system can be organized in two parts: 1) a first control stage that determines the total current reference that the load needs to maintain a specified voltage, 2) a second stage that distributes the total current among the different converters using CA. In the present paper, only the second stage is considered. The dynamics of the outer loop are assumed to be sufficiently slower than those of the current regulation loop using CA.

According to Kirchhoff's Voltage Law applied at the DC bus interconnection (See Fig. 2), the *average model* [21] gives:

$$\forall j \in \{1,2\}, \frac{di_j}{dt} = \frac{\alpha_j E_j}{L_j} - \frac{v}{L_j} \tag{28}$$

where α_j are the duty cycles of the buck converters and the input variables of the system to be controlled. Applying

Kirchhoff's Current Law, $i = i_1 + i_2$, where i is the total load current supplied to the RC circuit at the right side of Fig. 2. By choosing the state vector $\mathbf{X} = [i_1 \;\; i_2]^T$ and $\mathbf{U} = [\alpha_1 \;\; \alpha_2]^T$, the following state-space model is obtained:

$$\dot{\mathbf{X}} = \begin{bmatrix} E_1/L_1 & 0 \\ 0 & E_2/L_2 \end{bmatrix} \mathbf{U} + \begin{bmatrix} -1/L_1 \\ -1/L_2 \end{bmatrix} v = B\mathbf{U} + \mathbf{E} \quad (29)$$

The current that governs the voltage appearing on the load is the total current that the buck converters can deliver, so the output of the system (29) is $\mathbf{Y} = i_1 + i_2 = [1 \;\; 1]\mathbf{X} = C\mathbf{X}$. The discretization of (29) by matrix exponential gives (2) with $F = \mathbb{I}_2$, $G = BT_s$ and $H = T_s$.

In order to implement the CAI method described by (15), one needs to choose the dynamics to impose on the closed-loop system through the parameters F_M and Z_M. First, F_M is chosen according to the desired reference model. Then, Z_M is chosen for disturbance rejection, typically with dynamics faster than the reference tracking dynamics. The parameters considered for the simulation of the system are given in Table I. As in [10], the characteristics of the two converters are assumed to be different. The voltage v across the load is a variable to be controlled by an outer control loop with dynamics at least an order of magnitude slower than the inner loop. Thus, v is considered constant for the inner loop.

The desired 5% settling time in closed-loop is $T_{5\%} = 2.1$ ms for the reference tracking dynamics. Having only one output in this system: $n_y = 1$, the input-ouput dynamics in closed-loop will be of order $n_y = 1$ according to Theorem 3. Thus, the closed-loop stable pole placement is deduced, as given in Table I. The other pole Z_M influencing the dynamics of disturbance rejection is chosen slightly faster than F_M. In the realization of the *Allocation* block of Fig. 1, the EMOn method is used, which implements online optimization using the interior-point algorithm of [16] for quadratic optimization.

B. Simulation results: CAI vs. CA

The simulation tests are performed in the Matlab-Simulink environment in order to highlight the characteristics of CAI compared to CA. The step response of the system is triggered by a current reference of $\mathbf{y}^{ref}(t) = 16$ A appearing at $t = 3$ ms and a step-input disturbance on the control $\delta\mathbf{u}(t) = [0.25 \;\; 0.175]^T$ occurring from $t = 15$ ms.

TABLE I
SIMULATION TEST PARAMETERS

Meaning	Values
System Parameters	
Buck converters inductances	$L_1 = 1$ mH, $L_2 = 2$ mH
Buck converters voltage sources	$E_1 = E_2 = 24$ V
Duty cycles boundaries	$0 \leq \alpha_1 \leq 1$, $0.3 \leq \alpha_2 \leq 0.7$
Stabilized voltage across the load	$v = 12$ V
Load capacitor	$C = 5$ mF
Control Allocation with Integrator Tuning	
Settling time	$T_{5\%} = 2.1$ ms
Sampling time	$T_s = 0.1$ ms
Closed-loop poles (s-domain)	$P_s^+ = -1429$ rad/s
Closed-loop poles (z-domain)	$F_M = e^{T_s P_s^+} = 0.8669$
Disturbance rejection poles (z-domain)	$Z_M = 0.85$ $F_M = 0.7368$

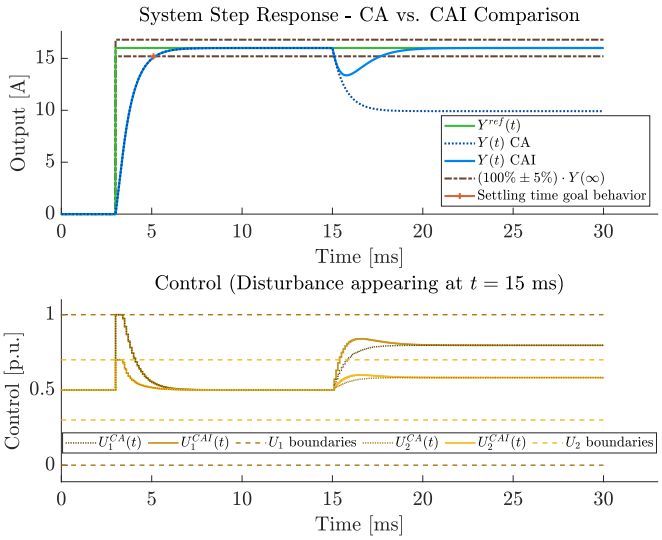

Fig. 3. Simulation results using the original Control Allocation (CA) architecture and the novel Control Allocation with Integrator (CAI) architecture.

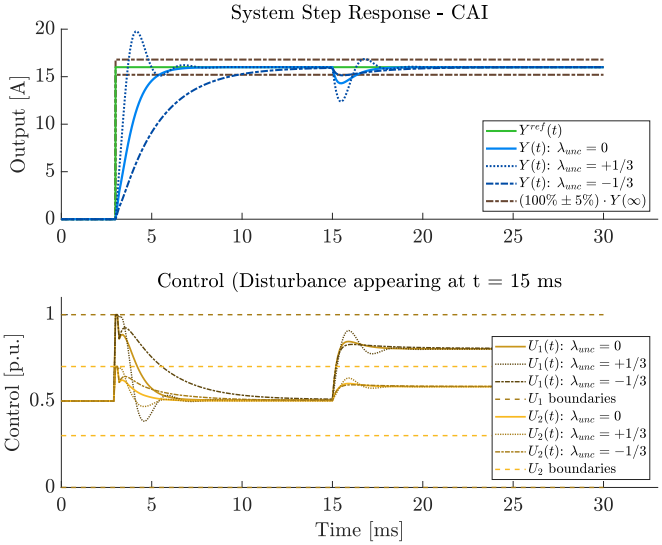

Fig. 4. Simulation results using the novel Control Allocation with Integrator (CAI) architecture under parametric uncertainties.

The simulation results in Fig. 3 show several behaviors: 1) CAI is well capable of disturbance rejection and it cancels the static error unlike CA, 2) the performance of the reference tracking dynamics meets the required settling time for both control methods. The small delay is due to the control saturating at the beginning of the simulation. Anti-windup methods are of importance to prevent the system from reaching undesired and unstable behaviors when saturating; however, they are not discussed in this paper and are part of future work.

A second simulation is designed to show how the properties of the CAI observed in the first simulation change when parametric uncertainties are present. For each matrix of the simulation model, a parameter variation is applied. Specifically, $(1 + \lambda_{unc})F$ replaces F. This modification is applied to the entire set of state-space model matrices. Three simulations are run: $\lambda_{unc} = 0$, $\lambda_{unc} = -1/3$ and for $\lambda_{unc} = +1/3$. Fig. 4

presents the simulations results.

Although parametric differences influence the dynamics of the closed loop, the CAI still guarantees zero static error and disturbance rejection. This means that the important benefit of using CAI over CA can also be ensured when experiencing some parametric uncertainties.

Note that the CAI method was also tested on a more complex system with higher order and larger number of inputs: the modular multilevel converter (MMC). See [12] for modelling details of this system. Although the results are not discussed here, the CAI algorithm was found to significantly improve the control performance, similarly to what was found for the simpler system (2 inputs, 1 output) of this paper.

IV. Conclusions

A new method was introduced that incorporates integral compensation in a multivariable model reference control scheme with CA. Important properties of the method were derived, such as the closed-loop transfer function matrix, the sensitivity function and the static error. Theoretical analysis and simulation results are found to be consistent: the addition of an integral action to the control allocation ensures elimination of static error and disturbance rejection. Simulation show that those capabilities hold also under small parametric uncertainties. The analysis made it possible to tune the desired response for reference tracking and disturbance rejection differently from the specification of a reference model. A major feature of the CAI, emphasized by Corollary 1, is that adding the integrator is transparent for the closed-loop response: no supplementary zero or pole appears due to the integrator and the same reference model than without the add-on is followed. Interestingly, the new method can be readily combined with existing methods for an important performance gain and little change of the control algorithm.

References

[1] E. G. Rynaski, "Experimental experience at Calspan," in *Restructurable Controls*, Aug. 1983, pp. 99–114, nasa Conference Publication 2277.

[2] T. B. Cunningham, "Robust reconfiguration for high reliability and survivability for advanced aircraft," in *Restructurable Controls*, Aug. 1983, pp. 43–80, nasa Conference Publication 2277.

[3] T. A. Johansen and T. I. Fossen, "Control allocation—A survey," *Automatica*, vol. 49, no. 5, pp. 1087–1103, May 2013.

[4] M. Bodson, "Evaluation of optimization methods for control allocation," *Journal of Guidance, Control, and Dynamics*, vol. 25, no. 4, pp. 703–711, Jul. 2002.

[5] F. Liao, K. Lum, J. L. Wang, and M. Benosman, "Constrained nonlinear finite-time control allocation," in *2007 American Control Conference*, Jul. 2007, pp. 3801–3806.

[6] S. A. Frost and M. Bodson, "Resource balancing control allocation," in *Proceedings of the 2010 American Control Conference*, Jun. 2010, pp. 1326–1331.

[7] S. S. Tohidi, Y. Yildiz, and I. Kolmanovsky, "Adaptive control allocation for over-actuated systems with actuator saturation," *IFAC-PapersOnLine*, vol. 50, no. 1, pp. 5492–5497, Jul. 2017.

[8] P. Kolaric, V. G. Lopez, and F. L. Lewis, "Optimal dynamic control allocation with guaranteed constraints and online reinforcement learning," *Automatica*, vol. 122, no. 109265, Dec. 2020.

[9] A. Bouarfa, M. Bodson, and M. Fadel, "An optimization formulation of converter control and its general solution for the four-Leg two-Level inverter," *IEEE Transactions on Control Systems Technology*, vol. 26, no. 5, pp. 1901–1908, Sep. 2018.

[10] J. Kreiss, M. Bodson, R. Delpoux, J.-Y. Gauthier, J.-F. Trégouët, and X. Lin-Shi, "Optimal control allocation for the parallel interconnection of buck converters," *Control Engineering Practice*, vol. 109, Apr. 2021.

[11] G. Le Goff, M. Fadel, and M. Bodson, "Modular polyphased full order current state-space model of the modular multilevel converter," in *2021 IEEE 19th International Power Electronics and Motion Control Conference (PEMC)*, Apr. 2021, pp. 132–139.

[12] ——, "Scalable Control Allocation: Real-time Optimized Current Control in the Modular Multilevel Converter for Polyphase Systems," in *2022 International Symposium on Power Electronics, Electrical Drives, Automation and Motion (SPEEDAM)*, Sorrento, Italy, Jun. 2022, pp. 712–718.

[13] K. Bordignon and W. Durham, "Null-space augmented solutions to constrained control allocation problems," in *Guidance, Navigation, and Control Conference*. American Institute of Aeronautics and Astronautics, Aug. 1995.

[14] J. Boskovic and R. Mehra, "Control allocation in overactuated aircraft under position and rate limiting," in *Proceedings of the 2002 American Control Conference*, vol. 1, May 2002, pp. 791–796 vol.1.

[15] O. Härkegård, *Backstepping and control allocation with applications to flight control*. Linköping: Univ, 2003.

[16] J. A. M. Petersen and M. Bodson, "Constrained quadratic programming techniques for control allocation," *IEEE Transactions on Control Systems Technology*, vol. 14, no. 1, pp. 91–98, Jan. 2006.

[17] J. Virnig and D. Bodden, "Multivariable control allocation and control law conditioning when control effectors limit," in *Guidance, Navigation, and Control Conference*. Scottsdale, AZ, U.S.A.: American Institute of Aeronautics and Astronautics, Aug. 1994.

[18] J. Buffington, "Tailless aircraft control allocation," in *Guidance, Navigation, and Control Conference*. American Institute of Aeronautics and Astronautics, Aug. 1997.

[19] L. Zaccarian, "Dynamic allocation for input redundant control systems," *Automatica*, vol. 45, no. 6, pp. 1431–1438, 2009.

[20] J. A. Petersen and M. Bodson, "Interior-Point Algorithms for Control Allocation," *Journal of Guidance, Control, and Dynamics*, vol. 28, no. 3, pp. 471–480, May 2005.

[21] S. Bacha, I. Munteanu, and A. I. Bratcu, *Power Electronic Converters Modeling and Control: with Case Studies*. London: Springer-Verlag, 2014.